https://doi.org/10.5194/egusphere-2023-2935
Preprint. Discussion started: 6 March 2024

Roles of oceanic ventilation and terrestrial outflow in the atmospheric non-methane hydrocarbons over the Chinese marginal seas

Jian Wang[1], Lei Xue[2], Qianyao Ma[1], Feng Xu[1], Gaobin Xu[1], Shibo Yan[1], Jiawei Zhang[3], Jianlong Li[1], Honghai Zhang[1,*], Guiling Zhang[1], Zhaohui Chen[4]

[1]Frontiers Science Center for Deep Ocean Multispheres and Earth System, Key Laboratory of Marine Chemistry Theory and Technology, Ministry of Education, and College of Chemistry and Chemical Engineering, Ocean University of China, Qingdao 266100, China

[2]Department of Chemistry, College of Environmental Science and Forestry, State University of New York, Syracuse, NY, 13210, United States

[3] Eco-Environmental Monitoring and Research Center, Pearl River Valley and South China Sea Ecology and Environment Administration, Ministry of Ecology and Environment, Guangzhou 510610, China

[4]Key Laboratory of Physical Oceanography, Ministry of Education, Ocean University of China, Qingdao 266100, China

* To whom correspondence should be addressed: honghaizhang@ouc.edu.cn

https://doi.org/10.5194/egusphere-2023-2935
Preprint. Discussion started: 6 March 2024

Abstract

Non-methane hydrocarbons (NMHCs) in the marine atmosphere have been extensively studied due to their important roles in regulating the atmospheric chemistry and climate. However, very little is known about the distribution and sources of NMHCs in the lower atmosphere over the marginal seas of China. Herein, we characterized the atmospheric NMHCs (C2-C5) in both the coastal cities and marginal seas of China in spring 2021, with a focus on identifying the sources of NMHCs in the coastal atmosphere. The NMHCs in urban atmospheres, especially for alkanes, were significantly higher compared to that in marine atmosphere, suggesting that terrestrial NMHCs may serve as an important reservoir/source of the marine atmosphere. A significant correlation was observed between the alkane concentrations and the distances from sampling sites to the nearest land or retention of air mass over land, indicating that alkanes in the marine atmosphere are largely influenced by terrestrial inputs through air-mass transport. For alkenes, a greater impact from oceanic emissions was determined due to the lower terrestrial concentrations, short atmospheric lifetime, and substantial sea-to-air fluxes of alkenes compared to alkanes (489 ± 454 vs 129 ± 106 nmol m^{-2} d^{-1}). As suggested by the positive matrix factorization, terrestrial inputs contributed to 89 % of alkanes and 69.6 % of alkenes in Chinese marginal seas, subsequently contributing to 84 % of the ozone formation potential associated with C2-C5 NMHCs. These findings underscore the significance of terrestrial outflow in controlling the distribution and composition of atmospheric NMHCs in the marginal seas of China.

Keywords: non-methane hydrocarbons, oceanic ventilation, terrestrial outflow, source apportionment

https://doi.org/10.5194/egusphere-2023-2935
Preprint. Discussion started: 6 March 2024

1 Introduction

Non-methane hydrocarbons (NMHCs), a significant subset of volatile organic compounds (VOCs), are acknowledged as key precursors to tropospheric ozone formation (Houweling et al., 1998; Solomon et al., 2005) and second organic aerosol (SOA) generation (Hallquist et al., 2009; Wu and Xie, 2018), playing a pivotal role in atmospheric chemistry. The presence and activity of NMHCs in the troposphere have far-reaching implications, not only influencing the dynamics of ozone and SOA formation but also significantly impacting air quality. These compounds are intricately linked to heightened human health risks as well as possessing indirect yet profound effects on the broader climate system through their interactions with various atmospheric processes (Yuan et al., 2018).

The emission of NMHCs into the atmosphere stems from an array of natural and anthropogenic processes. Oceanic sources of NMHCs predominantly entail the biogenic production of phytoplankton and photochemical degradation of dissolved organic matter (DOM) (Bonsang et al., 1992; Li et al., 2019; Riemer et al., 2000; Sahu et al., 2010). However, they are minimal when compared to terrestrial inputs. Previous estimates driven from a global VOCs emissions model formulated by Guenther et al. (1995) assign terrestrial sources a cumulative emission of 1141 Tg C $year^{-1}$, with oceanic emissions at merely 5 Tg C $year^{-1}$. A substantial amount of NMHCs originating from terrestrial sources (e.g., vehicular emissions, biomass combustion, industrial activities, and continental vegetation emissions) can be transported into the offshore atmosphere via air mass conveyance (Wang et al., 2005; Kato et al., 2007; Song et al., 2020). Subsequently, these supplementary terrestrial NMHCs will play a pivotal role in shaping the chemical composition of the offshore atmosphere and influencing local

https://doi.org/10.5194/egusphere-2023-2935
Preprint. Discussion started: 6 March 2024

environmental dynamics. Hence, to further understand the characteristics, variation, and origins of NMHCs in the offshore atmosphere, it is imperative to scrutinize oceanic emissions and meanwhile, it is necessary to figure out the effect of terrestrial outflow on nearshore NMHCs.

The Yellow Sea and the East China Sea are important parts of Chinese marginal seas, situated along the eastern coast of China where it is densely populated and has intensive industries. The rapid pace of Chinese development has seen a notable escalation in anthropogenic NMHCs emissions over recent decades (He et al., 2019). Presently, excessive NMHCs emissions and severe ozone pollution have emerged as urgent environmental challenges in China, particularly in highly urbanized and industrialized areas along the eastern coast (Liu et al., 2016; Zhang et al., 2018). The seasonal cycle of the Asian monsoon and diurnal fluctuations of sea-land breezes can facilitate the transport of terrestrial pollution to the marine atmosphere (Ding et al., 2004; Wang et al., 2003; Talbot et al., 2003; Russo et al., 2003). Additionally, eutrophication in coastal regions fosters the proliferation of phytoplankton, potentially augmenting the natural emissions of NMHCs. Consequently, conducting atmospheric investigations in the coastal region of eastern China is effective in revealing the potential effects of land-sea interactions on offshore atmospheric NMHCs.

In the spring of 2021, atmospheric samples were systematically collected from both coastal cities and marginal seas of China, providing representative insights into the characteristics of NMHCs (C2-C5) and facilitating discussion on the interplay between ocean emission and terrestrial outflow concerning atmospheric NMHCs. Ultimately, the contributions of diverse sources to NMHCs were quantified using the positive matrix factorization (PMF) model, with assistance from indications provided by other typical gases, mainly dimethyl sulfur (DMS), volatile halogenated compounds (VHCs),

https://doi.org/10.5194/egusphere-2023-2935
Preprint. Discussion started: 6 March 2024

and monocyclic aromatics.

2 Methods

2.1 Samples collection

The urban samples were collected from eight coastal cities in China from March 27 to April 1, 2021 (Fig. 1). Air samples were collected using fused silica-lined canisters (2.5 L), which were cleaned three times via a Canister Cleaning System (2101DS, Nutech) and were pumped into a negative pressure state before sampling. The sampling sites were selected at the top of high buildings to minimize contamination of particular point sources. Air samples were collected at 09:00 and 21:00 local time (UTC+8) aimed to represent the urban atmospheric conditions during the daytime and night, respectively. Note that night samples in Xiamen and Qinzhou were missing.

Oceanic air samples were collected aboard RV "*Dong Fang Hong 3*" during the voyage in the Yellow Sea and the East China Sea from April 17 to May 2, 2021. Nineteen oceanic air samples were collected on the top deck facing the wind when the ship was about to arrive at the station and started to slow down. Seawater samples were collected via prewashed Niskin bottles (12 L) incorporated into the Conductivity-Temperature-Depth Sensor Rosette (Seabird 911). Sampling details for urban and marine samples are shown in Table S4 and Table S5, respectively.

2.2 Analysis of air samples

All air samples were processed immediately after being brought back to the laboratory, using an Atmospheric Pre-concentrator System (8900DS, Nutech) coupled with a GC-MSD system (GC-7890A, MSD-5975, Agilent). The pretreatments of air

https://doi.org/10.5194/egusphere-2023-2935
Preprint. Discussion started: 6 March 2024

samples were as follows. First, the Atmospheric Pre-concentrator System was baked for 10 min to clean the interior instrument. Then trap 1 was cooled to -170 °C using liquid N_2 and a 300 mL air sample was pumped from the canister into trap 1 for the initial concentration of the target compounds, while N_2 and O_2 escaped due to their lower boiling points. After trap 2 was cooled to -50 °C, trap 1 was heated to 30 °C to transfer the target compounds from trap 1 to trap 2. Moisture and CO_2 were removed in the second concentration. Then, trap 2 was warmed up to transfer the target compounds into the last trap for cryofocusing (−175 °C). Finally, the last trap was instantaneously heated to 200 °C via gas bath heating, and the target compounds were delivered into the GC-MSD system by ultra-pure He.

For the parameter settings of GC-MSD, the temperature of the inlet, quadrupole, and ionization source was 150 °C, 150 °C, and 230 °C, respectively. The inlet was set to split mode with a ratio of 10:1. The flow rate of carrier gas (He) was set to 1.5 mL min^{-1} in the instant flow mode. Specific columns were selected to separate the NMHCs (Rt-Alumina BOND/KCl, Restek), monocyclic aromatics (DB-624, Agilent), DMS (CP7529, Agilent), and VHCs (DB-624, Agilent). Gas standards of NMHCs in N_2 (Linde Gases, Germany) were diluted to 0.1-1 ppb for identification and calibration. Details of temperature programming and detector parameters can be seen in Zou et al. (2021) and Li et al. (2019). The precision and detection limits for the trace gases in the present study were 1-7 % and 0.03-20.0 ppt, respectively (Table S1). Note that DMS and VHCs data in marine atmospheric samples were graciously provided by colleagues in the same laboratory. These data were only used as supporting information in the interpretation (e.g., correlation analysis) of our core dataset in this paper.

https://doi.org/10.5194/egusphere-2023-2935
Preprint. Discussion started: 6 March 2024

2.3 Analysis of seawater samples

C2-C5 NMHCs in seawater were measured immediately on board using a purge and trap system coupled with the gas chromatography equipped with a flame ionization detector (GC-FID, 7890B, Agilent). The purge and trap system was improved based on a previously self-designed device described by Li et al. (2019). Briefly, seawater was collected using a customized glass sampler (500 mL) and was connected to the inlet of the system. Then seawater was transformed into the extraction cell under the pressure of pure N_2 and was purged with pure N_2 bubble flow (250 mL min^{-1}). The moisture of the carrier gas condensed in a thin glass tube that was placed in a cold chamber (4-6 ℃) and the carbon dioxide was absorbed by the glass tube filled with Ascarite II (Merck). The targets were concentrated in a passivated stainless-steel tube immersed in liquid nitrogen for 26 mins. Then, the steel tube was heated by boiling water and immediately, the six-way valve was turned for the inlet situation. The concentrated target compounds were transferred into the Rt-Alumina BOND/KCl capillary column for separation and were determined by the FID. The parameters of the inlet, oven, and detector are shown in Table S2. The gas standard (Linde Gases, Germany) was diluted with ultra-pure N_2 to 10 ppb for identification and quantification. The instrumental blank was made to guarantee data reliability. The precision and detection limits were 3-6 % and 0.5-1.0 pmol L^{-1} (Table S3).

2.4 Calculation of sea-to-air flux

The sea-to-air flux of each NMHCs (F, nmol m^{-2} d^{-1}) was calculated using Eq. (1):

$$F = k \times (C_w - C_a \times H) \quad (1)$$

where k (m s^{-1}) is the gas transfer velocity described by Eq. (2); H is Henry's law constant; C_w (pmol L^{-1}) and C_a (ppb) are concentrations of each NMHCs in the

https://doi.org/10.5194/egusphere-2023-2935
Preprint. Discussion started: 6 March 2024

surface seawater (5 m depth) and atmosphere, respectively.

$$k = 0.31 \times u^2 \times (\frac{Sc}{660})^{-0.5} \quad (2)$$

where u (m s^{-1}) is the wind velocity at 10 m. Sc is the Schmidt number and is defined as Sc = v/D. v was the kinematic viscosity of seawater calculated by Eq. (3) (Wanninkhof, 1992). D is the gas diffusion coefficient related to temperature described by Eq. (4) (Wilke and Chang, 1955).

$$v = 1.052 + 1.300 \times 10^{-3} \times t + 5.000 \times 10^{-6} \times t^2 + 5.000 \times 10^{-7} \times t^3 \quad (3)$$

$$D = \frac{7.4 \times 10^{-8} (q \times M_b)^{0.5} \times T}{n_b \times V_a{}^{0.6}} \quad (4)$$

where t (℃) is the degree Celsius of seawater, q is the association factor of water, M_b (g mol^{-1}) is the molar weight of water, T (K) is the degree Kelvin of seawater, n_b is the dynamic viscosity of seawater and V_a is the molar volume at the boiling point.

2.5 Normalized concentrations and lifetime-weighted concentrations of NMHCs.

To effectively compare the NMHCs variation with respect to the distance from the sampling sites to the land (like Fig. 2d, f), we calculated the normalized concentration for each NMHCs (C_{Nor-i}) using Eq. (5).

$$C_{Nor-i} = \frac{C_i}{C_{max-i}} \quad (5)$$

where C_i is the concentration of gas *i* and C_{max-i} is the maximum of gas *i*.

A novel approach was employed to analyzed the correlation between the concentrations of various NMHCs and their sea-to-air fluxes. Concentrations were weighted according to the respective atmospheric •OH lifetime of each NMHCs. This was achieved by dividing the concentration of each NMHCs by its corresponding atmospheric •OH lifetime, yield a "lifetime-weighted concentration" for each NMHCs (C_{life-i}) (Eq. 6). This method provides a more nuanced understanding of the impact of

https://doi.org/10.5194/egusphere-2023-2935
Preprint. Discussion started: 6 March 2024

oceanic emission on NMHCs, taking into account not only their abundance but also their residence in the atmosphere.

$$C_{life-i} = \frac{C_i}{\tau_i} \quad (6)$$

where C_i is the atmospheric concentration of gas i, τ_i is the •OH lifetime of gas i. Approximate atmospheric lifetime of each NMHCs was calculated assuming an average [•OH] of 6×10^5 molecules cm^{-3} within 24 h at 288 K (Jobson et al., 1999), with specific data listed in Table 1.

2.6 Calculation of retention of air mass over land

To identify whether an air mass was mainly from terrestrial or oceanic regions, the retention ratio of the air mass over land (R_L) was calculated by Eq. (7).

$$R_L = \frac{\sum_{n=1}^{N_{land}} e^{-\frac{t_n}{48}}}{\sum_{n=1}^{N_{total}} e^{-\frac{t_n}{48}}} \quad (7)$$

Where N_{total} is the total number of trajectory endpoints (downloaded from NOAA Air Resources Laboratory HYSPLIT trajectory model https://www.arl.noaa.gov/). N_{land} is the total number of trajectory endpoints located over land, while t_n is the backward tracking time with the unit of hour and $e^{-\frac{t_n}{48}}$ is the weighting factor related to tracking time as the diffusion of air mass takes place along the transport path than in the nearby regions. As a result, the larger R_L value indicates that the air mass is more influenced by terrestrial transport and its source is more likely to be on land. Similar methods have been used to calculate the average residence time of sampled air masses in the Arctic (Willis et al., 2017) and identify the percentage of time spent by trajectories over different surface types in the Antarctic (Decesari et al., 2020). R_L values were calculated by three different time-scale trajectories (48h, 72h, and 96h). The mean R_L (n = 3) was finally applied to analyze the terrestrial influence on oceanic NMHCs,

https://doi.org/10.5194/egusphere-2023-2935
Preprint. Discussion started: 6 March 2024

mitigating the uncertainty caused by the trajectory with different time-scales.

2.7 Application of the PMF model

PMF model introduced in detail in the study of (Paatero and Tapper, 1994) was applied to analyze the data of atmospheric NMHCs in the Yellow Sea and South China Sea. Based on a matrix consisting of the concentrations of diverse chemical species, the objective of PMF is to determine the number of NMHCs source factors, the chemical composition profile of each factor, and the contribution of each factor to species. In the application of the PMF model, the significance of missing data in the matrix was decreased by using the species median. The uncertainty for normal data was estimated as 20 % of the NMHCs concentrations because the analytical uncertainty was not available (Buzcu and Fraser, 2006). In this analysis, the model ran 20 times and we selected the result with the minimum "Q value". Besides, approximately 94 % of the scaled residuals given by PMF ranged from -3 to 3 (Fig. S1), suggesting a reasonable fit of the model result.

3 Results and discussion

3.1 Atmospheric concentrations of NMHCs in coastal cities and coastal seas of China

To clarify, NMHCs determined in this study were separated into two groups for further discussion based on their distinctly different atmospheric reactivity and lifetimes: alkanes (long lifetime, 8.2-78 d) and alkenes (short lifetime, 0.19-2.3 d). In urban atmosphere (n = 14), the mean (range) concentration of ethane, propane, i-butane, and n-butane was 2.26 (0.277-5.72), 2.95 (0.149-20.1), 2.57 (BD-27.6), and 3.29 (0.018-

https://doi.org/10.5194/egusphere-2023-2935
Preprint. Discussion started: 6 March 2024

30.2) ppb, respectively (Table 1). Alkanes combined accounted for ~76 %-99 % of total NMHCs measured in this study, which agrees with previous studies reporting alkanes as the dominant NMHCs in the urban atmosphere of China e.g., 43.7 % (Song et al., 2007), and > 50 % (Li et al., 2015). For alkene species in the urban atmosphere (n = 14), the mean (range) of ethylene, propylene, and isoprene was 0.180 (0.035-0.390), 0.036 (BD-0.129), and 0.046 (0.006-0.250) ppb, respectively.

Similarly, alkanes were also dominant components in the marine atmosphere, accounting for ~86 %-95 % of NMHCs. In the marine atmosphere (n = 19), the mean (range) concentration of ethane, propane, i-butane, n-butane, ethylene, propylene, and isoprene was 1.24 (0.686-1.72), 0.822 (0.226-1.79), 0.283 (BD-1.17), 0.256 (0.025-0.694), 0.151 (0.028-0.295), 0.033 (0.022-0.060), and 0.008 (BD-0.043) ppb, respectively. These values were comparable to those reported in the Bengal Bay (Sahu et al., 2011) and the Northwest Pacific Ocean (Li et al., 2019) (Table S6). Alkanes in the urban atmosphere were on average more than four times higher than those in the marine atmosphere, while no significant difference was observed for concentrations of alkenes between urban and marine air (t = 2.224, p = 0.156) (Fig. 2a, b). This suggests that the terrestrial alkanes may potentially serve as a reservoir/source of the alkanes in the marine atmosphere through the transport of terrestrial air mass.

3.2 Atmospheric NMHCs variability vs. estimated lifetime

The standard deviation of the natural logarithm of the NMHCs mixing ratios (S_{lnx}) was established to correlate to their •OH lifetime (τ) in the atmosphere following an exponential function of $S_{lnx} = A\tau^{-b}$ (Jobson et al., 1998), where A and b are fitting parameters. A b value approaching zero suggests that the NMHCs variability is primarily controlled by local emission fluctuations while a b value of 1 indicates the

https://doi.org/10.5194/egusphere-2023-2935
Preprint. Discussion started: 6 March 2024

minimal impact of local emissions, with the variability predominantly controlled by the extent of photochemical reactions.

Employing the analytical framework in Jobson et al. (1998), we analyzed our atmospheric NMHCs data from urban areas and the Chinese marginal seas. The derived *b* value for urban areas was 0.05 (Fig. 3a), suggesting that atmospheric NMHCs in coastal cities were mainly controlled by local emissions. In the marine atmosphere, the *b* value was 0.26 (Fig. 3b) which was comparable to values reported for Gosan (0.30) (Wong et al., 2007) and continental outflow from southern China (0.31) (Wang et al., 2005), but it was significantly lower than the values for Ogasawara (0.43) (Kato et al., 2004), the Northwest Indian Ocean (0.40) (Warneke and De Gouw, 2001), and the South China Sea (0.42) (Wang et al., 2005). The *b* value of 0.26 in the atmosphere over the Chinese marginal suggests that the NMHCs composition in nearshore atmosphere is influenced both by local oceanic emissions and the remote sources from the continent. As sites closer to the source position tend to have lower *b* values, the Yellow Sea and the East China Sea experience a more pronounced influence from terrestrial pollution sources compared to Ogasawara, the South China Sea, and the Northwest Indian Ocean.

3.3 Terrestrial influence on marine atmospheric NMHCs variation

Given the discernible impact of terrestrial input on the spatial distributions and variabilities of marine atmospheric NMHCs, we further elucidated the role of terrestrial outflow in shaping marine atmospheric NMHCs levels. This examination focused on three key factors: distance from the sampling site to the land, retention of air mass over land, and transport time of air mass.

https://doi.org/10.5194/egusphere-2023-2935
Preprint. Discussion started: 6 March 2024

Distance from the sampling site to the land

The distances from the oceanic sampling sites to the nearest land spanned from 13.9 to 331 km, with an average of 123 km (Table S9). Significant correlations were observed between the distances and concentrations of ethane (r = -0.553, n = 19, p = 0.014), propane (r = -0.605, n = 19, p = 0.006), i-butane (r = -0.513, n = 19, p = 0.025), and n-butane (r = -0.573, n = 19, p = 0.010). When plotted against the distances, the concentrations of alkanes combined decreased with the increasing distance (Fig. 2c), and different species exhibited distinctly specific decreasing rates (Fig. 2d). Since the concentrations between different NMHCs species varied considerably, the normalized concentrations were employed to fit an attenuation equation ($y = Ae^{-tx}+y_0$) for each species. As evident in Fig. 2d, the attenuation coefficients for ethane, propane, i-butane, and n-butane were 0.003, 0.030, 0.031, and 0.022, respectively. These coefficients were correlated with their atmospheric reactivities. Species with lower reactivity and longer lifetimes, such as ethane (with a lifetime of 78 d), have the lowest attenuation coefficient. This implies that long-lifetime species could be affected by the terrestrial input even at a more remote marine site. Terrestrial influences on propane, i-butane, and n-butane were discernible only in areas much closer to land, as their concentrations stabilized at low values beyond a distance of around 100 km (Fig. 2d).

Retention of air mass over land

A larger retention of air mass over land (R_L) has previously been suggested to serve as an indicator of a greater terrestrial influence (Zhou et al., 2021). To mitigate the uncertainty derived from varying time-scale trajectories, we calculated the R_{L-mean} based on 48, 72, and 96-hour backward trajectories. R_{L-mean} ranged from 0.10 to 0.96 (Table S9). When plotted against R_{L-mean}, a linear relationship was observed between

https://doi.org/10.5194/egusphere-2023-2935
Preprint. Discussion started: 6 March 2024

the concentrations of NMHCs combined and R_{L-mean}, with a slope of 2.51 (Fig. 4a). A statistically significant correlation (r = 0.599, n = 19, p = 0.007) was observed when only plotting alkanes with R_{L-mean}. However, the correlation between alkenes and R_{L-mean} was statistically insignificant (r = 0.248, n = 19, p = 0.306).

Transport time of air mass

The transport time of air mass was estimated as the interval from the last point of the trajectory contacting the continent to the moment when the air mass reached the sampling location, as detailed by Kato et al. (2001). These times ranged from 4 to 81 h, with an average of 30 h (Table S9). A shorter air mass transport time signifies a stronger terrestrial influence, as NMHCs within the air mass undergo further oxidation and dispersion over time. Total NMHCs concentrations exhibited a significant decrease with the increase of air mass transport time, characterized by a slope of -0.04 (Fig. 4d). Alkanes displayed a steeper decline, indicated by a slope of -0.0079 (Fig. 4e) compared to alkenes (-0.0038, Fig. 4f). However, similar to the analysis of R_L, the correlation between the air mass transport time and alkenes was statistically insignificant (r = 0.248, n = 19, p = 0.306).

Overall, the analysis above suggests that the terrestrial input plays an important role in driving the variability observed for the atmospheric NMHCs over the marginal seas of China. In particular, a stronger terrestrial impact was determined for the alkanes based on the larger slopes from linear regression analysis and the significant correlations with terrestrial indicators. In contrast, no discernible trend was found for alkenes when plotting their concentrations against the distance from sampling sites to the coastline (Fig. 2e, f). There was no significant correlation between alkenes and R_L or air mass transport time. Therefore, the variability of alkenes in the coastal

https://doi.org/10.5194/egusphere-2023-2935
Preprint. Discussion started: 6 March 2024

atmosphere seems to be weakly impacted by the terrestrial sources when compared to alkanes. We attribute this to two main factors. First, the mean concentration of alkenes in the urban air was only 1.4 times of that in marine air, whereas it was 5.4 times for alkanes. Alkenes undergo more rapid oxidation due to their higher reactivities compared to alkanes during air mass transport. Secondly, oceanic ventilation may play a more substantial role in affecting marine alkenes (discussed in section 3.4).

3.4 Oceanic impact on marine atmospheric NMHCs composition

Sea-to-air fluxes of NMHCs

The mean (range) of sea-to-air fluxes of ethane, propane, i-butane, n-butane, ethylene, propylene, and isoprene was 44.6 (0.2-118), 41.5 (0.2-157), 31.7 (0.1-146), 10.9 (-0.8-96.1), 321 (1.7-775), 56.1 (0.2-212), and 112 (0.5-468) nmol m^{-2} d^{-1}, respectively, in the Yellow Sea and the East China Sea (Table 1). These values were comparable to those reported in Chinese marginal seas (Wu et al., 2021; Li et al., 2021) and 23-38°N Atlantic Ocean (Tran et al., 2013), but were larger than those reported values in the North Sea (Broadgate et al., 1997) and the Northwest Pacific Ocean (Li et al., 2019; Wu et al., 2023) (Table S10).

The mean of sea-to-air fluxes of the total observed NMHCs was 698 ± 607 nmol m^{-2} d^{-1} in areas within 100 km from the coastline, which was relatively higher than that in the regions beyond 100 km (480 ± 481 nmol m^{-2} d^{-1}). These elevated fluxes in the sea areas closer to land could be attributed to the influence of phytoplankton biomass and chromophoric dissolved organic matter (CDOM). Seawater NMHCs are not only directly synthesized by phytoplankton (Ratte et al., 1995), but they can also be emitted through the photochemical degradation of CDOM (Ratte et al., 1993; Lee and Baker, 1992). To substantiate our findings, we analyzed the monthly Chl-*a* concentration and

https://doi.org/10.5194/egusphere-2023-2935
Preprint. Discussion started: 6 March 2024

the absorption coefficient at 443 nm of seawater in April 2021 from the remote sensing dataset from the NASA Ocean Color data service (https://oceancolor.gsfc.nasa.gov/) (Fig. S2). The mean (±SD) of Chl-*a* concentrations was 2.83±1.17 and 1.68±1.44 μg L^{-1} in the areas within and beyond 100 km from coastline, respectively. Correspondingly, the mean (±SD) of seawater absorption coefficients at 443 nm was at 0.124±0.060 and 0.069 ± 0.040 m^{-1}, respectively. Hence, the heightened phytoplankton biomass and enriched photoreaction substrate collectively enhanced both the biological production and abiotic formation of NMHCs, consequently resulting in a pronounced NMHCs emission in nearshore regions.

Assessing the effect of oceanic emission on NMHCs

Prior to delving into the correlation between oceanic emissions and NMHCs concentrations, it is imperative to acknowledge the influence of different gases' reactivity on this relationship. For instance, ethane possesses an atmospheric lifetime of approximately 78 d at 24 h [•OH] concentration of 6×10^5 molecules cm^{-3}. This means all ethane emitted from the ocean within this period to potentially contribute to the accumulation of atmospheric ethane. Conversely, isoprene, with a much shorter lifetime of only 0.2 d, emitted within a very brief window can impact its atmospheric level. Thus, to mitigate the impact of varying reactivity among the different gas species, we calculated the life-weighted concentrations of each NMHCs according to their atmospheric lifetime (introduced in section 2.5). This novel method is more nuanced to assess the impact of oceanic emission on atmospheric NMHCs, as it acknowledging not only their abundance but also their residence in the atmosphere.

In spite of the elevated oceanic emission of NMHCs within the 100 km from land, its impact on atmospheric NMHCs composition was comparatively weak displaying a

https://doi.org/10.5194/egusphere-2023-2935
Preprint. Discussion started: 6 March 2024

slope of 0.0187 (Fig. 5c), which was lower than the fitted result of the dataset in areas beyond 100 km from land with a slope of 0.0415 (Fig. 5d). This could be attributed to the disturbance of terrestrial outflow in nearshore areas, mitigating the direct impact of oceanic emission on NMHCs. As it extended further from the land, the terrestrial influence diminished. This, in turn, strengthens the regulatory impact of oceanic emission on atmospheric NMHCs levels.

In addition, the average flux of total alkenes across the entire region was 163 ± 221 nmol m^{-2} d^{-1}, which was approximately 5 times higher than that of alkanes (32.2 ± 37.5 nmol m^{-2} d^{-1}). This substantial discrepancy indicates that alkanes and alkenes are certainly influenced differently by oceanic emissions. The correlation between the lifetime-weighted concentrations of alkenes and their fluxes was statistically significant ($r = 0.548$, $n = 57$, $p < 0.001$), while it was insignificant for alkanes ($r = 0.113$, $n = 76$, $p = 0.329$). When specific species of alkanes (Fig. 5e) and alkenes (Fig. 5f) were separately plotted against their sea-to-air fluxes, alkenes exhibited a steeper slope of 0.0072 compared to the slope of 0.0044 for alkanes. This signifies that oceanic emission has a more significant impact on atmospheric alkenes compared to alkanes, which verifies our hypothesis as stated at the end of section 3.3.

3.5 Identification and apportionment of the sources of marine atmospheric NMHCs

Source identification

Since the chemical compositions are largely controlled by the sources of emissions, specific ratios of hydrocarbons have been widely employed to identify the sources of NMHCs (Gilman et al., 2013; Rossabi and Helmig, 2018). For instance, elevated iso-pentane/n-pentane ratios are indicative of the heavy influence of vehicular emissions

https://doi.org/10.5194/egusphere-2023-2935
Preprint. Discussion started: 6 March 2024

(2.2-3.8) and gasoline fuel evaporation (1.8-4.6) (Gentner et al., 2009; Jobson et al., 2004; Liu et al., 2008; Russo et al., 2010). Conversely, the lower ratios indicate the importance of tropical forest fires (0.43-0.57) (Andreae and Merlet, 2001; Rossabi and Helmig, 2018), natural and oil gas operations (0.81-1.1) (Gilman et al., 2013; Swarthout et al., 2013), and marine vessel exhaust (1.59-1.71) (Bourtsoukidis et al., 2019) in controlling the chemical composition of NHMCs. In this study, a significant correlation was observed between i-pentane and n-pentane ($r = 0.67$, $p < 0.01$) (Fig. 6), and the i-pentane/n-pentane ratio spans a wider range from 0.89 to 2.46, suggesting that the composition of NMHCs in the marginal seas of China is controlled by multiple sources e.g., natural and oil gas operations, marine vessel exhaust, vehicular emissions, and gasoline evaporation.

Furthermore, propane, i-butane, and n-butane exhibited strong intercorrelations ($r = 0.52$-0.95, $p < 0.05$). They also displayed strong correlations with ethane, i-pentane, and n-pentane ($r = 0.55$-0.98, $p < 0.05$). These alkanes were recognized as the primary components of liquid petroleum gases (Blake and Rowland, 1995), extensively utilized as fuel in taxis, private cars, and public buses in China (Guo et al., 2017; Zhang et al., 2015). Notably, C3-C5 alkanes also exhibited significant correlations with ethane ($r = 0.55$-0.72, $p < 0.05$) and carbon monoxide ($r = 0.59$-0.81, $p < 0.05$), while ethane and carbon monoxide are acknowledged tracers for fossil fuel or biomass/biofuel combustion and incomplete combustion, respectively (Lai et al., 2010; Tang et al., 2009; Parrish et al., 2009). This indicated the contribution of vehicular emissions of liquid petroleum gases and combustion of fossil fuel or biomass to light alkanes. Additionally, strong correlations were observed among monocyclic aromatics (benzene, toluene, ethylbenzene) ($r = 0.67$-0.83, $p < 0.05$). This finding was consistent with recent emission inventory research identifying monocyclic aromatics as significant

https://doi.org/10.5194/egusphere-2023-2935
Preprint. Discussion started: 6 March 2024

constituents of ship exhaust (Xiao et al., 2018b; Wu et al., 2019). As for oceanic emissions, we have presented the sea-to-air fluxes of NMHCs and discussed the significant effect of oceanic emissions on NMHCs in Section 3.4. Multiple studies highlighted that the ocean is one of the important sources of these gases (Kato et al., 2007; Li et al., 2019; Mallik et al., 2013; Sahu et al., 2010; Rudolph and Johnen, 1990).

Source apportionment

The potential sources of the atmospheric NMHCs and their respective contributions to each category were determined using the PMF model. Four isolate factors were extracted according to their composition profiles depicted in Fig. 7a. These factors, including industrial production, exhaust emission, terrestrial vegetation, and oceanic ventilation, were identified based on chemical profiles in literature.

Propane, i-butane, n-butane, i-pentane, n-pentane, and CFC-11 showed strong loadings (> 70 %) on factor 1. The presence of propane, butanes, and pentanes suggests the influence of the refinery activities (Buzcu and Fraser, 2006). Additionally, propane has been recognized as a characteristic NMHCs derived from natural gas emissions and butane is indicative of liquefied petroleum gas (LPG) (Guo et al., 2011; Tsai et al., 2006; Hui et al., 2018; Ho et al., 2009). Moreover, CFC-11 is a typical artificial industrial product. Subsequently, factor 1 was identified as a factor relating to industrial activities.

The profile of factor 2 showed strong loadings of benzene (72 %), toluene (57 %), and ethylbenzene (64 %), along with moderate impacts of ethylene (34 %) and propylene (32 %). Benzene emissions are notably associated with vehicle exhaust (Zhang et al., 2013; Zhang et al., 2016) and considerable fractions of aromatics can be emitted from ship exhaust during both berthing and cruising (Cooper, 2005; Xiao et al., 2018a). C2-C4 alkenes could stem from ship emissions in the open ocean (Eyring et al.,

https://doi.org/10.5194/egusphere-2023-2935
Preprint. Discussion started: 6 March 2024

2005). Therefore, factor 2 can be potentially assigned as a source of the exhaust emissions of vehicles and ships.

Factor 3 was assigned as oceanic ventilation due to elevated percentages of DMS (74 %) and $CHBr_3$ (53 %), considering the dominant contributions of ocean emission to DMS (Lana et al., 2011; Lee and Brimblecombe, 2016) and $CHBr_3$ (Quack and Wallace, 2003; Ashfold et al., 2014). Factor 4 was mainly characterized by a high percentage of isoprene (68 %), an indicator of biogenic emission from terrestrial vegetation (Guenther et al., 2006; Wu et al., 2016). However, given isoprene's high reactivity, this factor should be treated cautiously and regarded as a lower limit (Fujita, 2001). Although its short atmospheric lifetime hinders long-range transport, the minimum air mass transport time from land to the oceanic station was four hours in this study, implying the potential for terrestrial isoprene to reach the nearshore atmosphere.

According to the results of the PMF model analysis, the dominant source of atmospheric alkanes in the Chinese marginal seas was industrial activities (0.253 ppb, 60.8 %), followed by exhaust emissions (0.095 ppb, 23 %). Contributions from terrestrial vegetation emission (0.049 ppb, 11 %) and oceanic ventilation (0.021 ppb, 5.2 %) were relatively smaller. Furthermore, exhaust emissions (0.017 ppb, 32.5 %), industrial activities (0.017 ppb, 31 %), and ocean ventilation (0.016 ppb, 30.4 %) contribute almost equally to atmospheric alkenes. Collectively, these three factors constitute the main sources of alkenes (93.8 %), whereas the contribution from terrestrial vegetation is minimal, at merely 6.2 %. Particularly, the contribution of terrestrial sources to alkanes (89 %) is greater than that to alkenes (69.6 %), while the contribution of ocean emission to alkenes (30.4 %) is greater than that to alkanes (5.2 %). This is consistent with the conclusions in section 3.3 and section 3.4.

To assess the environmental implications of different sources, the ozone formation

https://doi.org/10.5194/egusphere-2023-2935
Preprint. Discussion started: 6 March 2024

potential (OFP) of NMHCs was calculated using $OFP = MIR \times C$, where *MIR* depicts the maximum incremental reactivity and *C* represents the concentration of NMHCs (Carter, 1994). Specific data can be seen in supplementary Table S11. The contributions of different factors to the OFP are as follows: industrial activities (2.30 μg m^{-3}, 56 %), exhaust emissions (0.87 μg m^{-3}, 21 %), oceanic ventilation (0.64 μg m^{-3}, 16 %), and terrestrial vegetation emissions (0.27 μg m^{-3}, 7 %). Notably, terrestrial sources collectively accounted for 89 % of alkanes and 69.6 % of alkenes within the coastal marine atmosphere of China. Furthermore, these terrestrial factors contributed 84 % of the OFP associated with C2-C5 NMHCs. These findings highlight that terrestrial outflow substantially constitutes the atmospheric NMHCs and plays a significant role in regulating air quality in nearshore environments.

4 Conclusions

Our study characterized the atmospheric NMHCs in both coastal cities and Chinese marginal seas, and determined that both oceanic ventilation and terrestrial inputs play important roles in controlling the distribution and chemical composition of NMHCs in the coastal atmosphere of China.

Alkanes were the dominant NMHCs both in urban and nearshore atmosphere, and the atmospheric concentrations of alkanes were significantly higher in coastal cities compared to coastal seas, showing the potential of terrestrial alkanes as a source of alkanes in the marine atmosphere through transport. Generally, alkane concentrations tended to be higher in cases: sampling sites closer to land, longer retention of air mass over land, and shorter air mass transport time from land to sampling site. However, these effects could not apply to alkenes due to their higher reactivities and the substantial sea-to-air fluxes. Additionally, the impact of oceanic emissions on NMHCs

https://doi.org/10.5194/egusphere-2023-2935
Preprint. Discussion started: 6 March 2024

composition was more pronounced in areas beyond 100 km from land compared to areas within 100 km, because the terrestrial input gradually diminishes along the direction towards the open ocean.

Combining the outcomes of the PMF model and chemical profiles of diverse sources in the literature, we extracted four isolated sources of NMHCs in the nearshore atmosphere. Terrestrial sources (including industrial activities, vehicular exhaust, and vegetation emission) primarily constitute the NMHCs in the nearshore atmospheres, further contributing 84 % to the OFP associated with C2-C5 NMHCs. This highlights the significant influence of terrestrial outflow on the distribution and composition of NMHCs in the nearshore atmosphere of China, emphasizing the necessity for a comprehensive understanding of both natural and anthropogenic emissions of NMHCs.

Code and data availability

Data presented in this paper are publicly available at Figshare via https://doi.org/10.6084/m9.figshare.24722286. The remote-sensing datasets of Chl-*a* and total absorption at 443 nm are available at https://oceancolor.gsfc.nasa.gov. Code to calculate retention of air mass over land can be download from https://doi.org/10.1029/2021JD034960 (Zhou et al., 2021).

Competing interests

The authors declare that they have no conflict of interest.

https://doi.org/10.5194/egusphere-2023-2935
Preprint. Discussion started: 6 March 2024

Author contributions

Honghai Zhang and Jian Wang designed the investigation and experiments. Jian Wang, Qianyao Ma, Feng Xu, Gaobin Xu, Shibo Yan, Jiawei Zhang, and Jianlong Li collected and determined the samples. Jian Wang analyzed the data and wrote the manuscript. Honghai Zhang, Lei Xue, Zhaohui Chen, and Guiling Zhang reviewed and revised the manuscript.

Acknowledgments

We thank the chief scientist, captain, and crews of the R/V '*Dong Fang Hong 3*' for assistance and cooperation during the investigation. We would like to acknowledge the NOAA Air Resource Laboratory for the provision of the HYSPLIT trajectory model used in this study and the NASA Ocean Color data service for provision of the remote-sensing dataset of Chl-*a* and total absorption at 443 nm in this study region.

Financial support

This work was financially supported by the National Natural Science Foundation of China (42276042, 41876082, and 42006044); the Laoshan Laboratory (LSKJ 202201701), the Fundamental Research Funds for the Central Universities (202372001 and 202072001).

References

Andreae, M. O. and Merlet, P.: Emission of trace gases and aerosols from biomass burning, Glob.

https://doi.org/10.5194/egusphere-2023-2935
Preprint. Discussion started: 6 March 2024

Biogeochem. Cycle, 15, 955-966, https://doi.org/10.1029/2000GB001382, 2001.

Ashfold, M. J., Harris, N. R. P., Manning, A. J., Robinson, A. D., Warwick, N. J., and Pyle, J. A.: Estimates of tropical bromoform emissions using an inversion method, Atmos. Chem. Phys., 14, 979-994, https://doi.org/10.5194/acp-14-979-2014, 2014.

Atkinson, R., Baulch, D. L., Cox, R. A., Hampson, R. F., Kerr, J. A., Rossi, M. J., and Troe, J.: Evaluated kinetic, photochemical and heterogeneous data for atmospheric chemistry .5. Iupac subcommittee on gas kinetic data evaluation for atmospheric chemistry, J. Phys. Chem. Ref. Data, 26, 521-1011, https://doi.org/10.1063/1.556011, 1997.

Blake, D. R. and Rowland, F. S.: Urban leakage of liquefied petroleum gas and its impact on Mexico City air quality, Science, 269, 953-956, https://doi.org/10.1126/science.269.5226.953, 1995.

Bonsang, B., Polle, C., and Lambert, G.: Evidence for marine production of isoprene, Geophys. Res. Lett., 19, 1129-1132, https://doi.org/10.1029/92GL00083, 1992.

Bourtsoukidis, E., Ernle, L., Crowley, J. N., Lelieveld, J., Paris, J. D., Pozzer, A., Walter, D., and Williams, J.: Non-methane hydrocarbon (c2-c8) sources and sinks around the Arabian Peninsula, Atmos. Chem. Phys., 19, 7209-7232, https://doi.org/10.5194/acp-19-7209-2019, 2019.

Broadgate, W. J., Liss, P. S., and Penkett, S. A.: Seasonal emissions of isoprene and other reactive hydrocarbon gases from the ocean, Geophys. Res. Lett., 24, 2675-2678, https://doi.org/10.1029/97GL02736, 1997.

Buzcu, B. and Fraser, M. P.: Source identification and apportionment of volatile organic compounds in Houston, TX, Atmos. Environ., 40, 2385-2400, https://doi.org/10.1016/j.atmosenv.2005.12.020, 2006.

Carter, W. P. L.: Development of ozone reactivity scales for volatile organic compounds, J. Air Waste Manag. Assoc., 44, 881-899, https://doi.org/10.1080/1073161X.1994.10467290, 1994.

Cooper, D. A.: Hcb, pcb, pcdd and pcdf emissions from ships, Atmos. Environ., 39, 4901-4912, https://doi.org/10.1016/j.atmosenv.2005.04.037, 2005.

Decesari, S., Paglione, M., Rinaldi, M., Dall'Osto, M., Simó, R., Zanca, N., Volpi, F., Facchini, M. C., Hoffmann, T., Götz, S., Kampf, C. J., O'Dowd, C., Ceburnis, D., Ovadnevaite, J., and Tagliavini, E.: Shipborne measurements of antarctic submicron organic aerosols: An NMR

https://doi.org/10.5194/egusphere-2023-2935
Preprint. Discussion started: 6 March 2024

perspective linking multiple sources and bioregions, Atmos. Chem. Phys., 20, 4193-4207, https://doi.org/10.5194/acp-20-4193-2020, 2020.

Ding, A., Wang, T., Zhao, M., Wang, T., and Li, Z. K.: Simulation of sea-land breezes and a discussion of their implications on the transport of air pollution during a multi-day ozone episode in the Pearl River Delta of China, Atmos. Environ., 38, 6737-6750, https://doi.org/10.1016/j.atmosenv.2004.09.017, 2004.

Eyring, V., Kohler, H. W., van Aardenne, J., and Lauer, A.: Emissions from international shipping: 1. The last 50 years, J. Geophys. Res.-Atmos., 110, https://doi.org/10.1029/2004JD005619, 2005.

Fujita, E. M.: Hydrocarbon source apportionment for the 1996 Paso del Norte Ozone Study, Sci. Total Environ., 276, 171-184, https://doi.org/10.1016/S0048-9697(01)00778-1, 2001.

Gentner, D. R., Harley, R. A., Miller, A. M., and Goldstein, A. H.: Diurnal and seasonal variability of gasoline-related volatile organic compound emissions in riverside, California, Environ. Sci. Technol., 43, 4247-4252, https://doi.org/10.1021/es9006228, 2009.

Gilman, J. B., Lerner, B. M., Kuster, W. C., and de Gouw, J. A.: Source signature of volatile organic compounds from oil and natural gas operations in Northeastern Colorado (vol 47, pg 1297, 2013), Environ. Sci. Technol., 47, 10094-10094, https://doi.org/10.1021/es4036978, 2013.

Guenther, A., Karl, T., Harley, P., Wiedinmyer, C., Palmer, P. I., and Geron, C.: Estimates of global terrestrial isoprene emissions using MEGAN (model of emissions of gases and aerosols from nature), Atmos. Chem. Phys., 6, 3181-3210, https://doi.org/10.5194/acp-6-3181-2006, 2006.

Guenther, A., Hewitt, C. N., Erickson, D., Fall, R., Geron, C., Graedel, T., Harley, P., Klinger, L., Lerdau, M., McKay, W. A., Pierce, T., Scholes, B., Steinbrecher, R., Tallamraju, R., Taylor, J., and Zimmerman, P.: A global-model of natural volatile organic-compound emissions, J. Geophys. Res.-Atmos., 100, 8873-8892, https://doi.org/10.1029/94JD02950, 1995.

Guo, H., Cheng, H. R., Ling, Z. H., Louie, P. K. K., and Ayoko, G. A.: Which emission sources are responsible for the volatile organic compounds in the atmosphere of Pearl River Delta?, J. Hazard. Mater., 188, 116-124, https://doi.org/10.1016/j.jhazmat.2011.01.081, 2011.

Guo, H., Ling, Z. H., Cheng, H. R., Simpson, I. J., Lyu, X. P., Wang, X. M., Shao, M., Lu, H. X., Ayoko, G., Zhang, Y. L., Saunders, S. M., Lam, S. H. M., Wang, J. L., and Blake, D. R.:

https://doi.org/10.5194/egusphere-2023-2935
Preprint. Discussion started: 6 March 2024

Tropospheric volatile organic compounds in China, Sci. Total Environ., 574, 1021-1043, https://doi.org/10.1016/j.scitotenv.2016.09.116, 2017.

Hallquist, M., Wenger, J. C., Baltensperger, U., Rudich, Y., Simpson, D., Claeys, M., Dommen, J., Donahue, N. M., George, C., Goldstein, A. H., Hamilton, J. F., Herrmann, H., Hoffmann, T., Iinuma, Y., Jang, M., Jenkin, M. E., Jimenez, J. L., Kiendler-Scharr, A., Maenhaut, W., McFiggans, G., Mentel, T. F., Monod, A., Prevot, A. S. H., Seinfeld, J. H., Surratt, J. D., Szmigielski, R., and Wildt, J.: The formation, properties and impact of secondary organic aerosol: Current and emerging issues, Atmos. Chem. Phys., 9, 5155-5236, https://doi.org/10.5194/acp-9-5155-2009, 2009.

He, Z. R., Wang, X. M., Ling, Z. H., Zhao, J., Guo, H., Shao, M., and Wang, Z.: Contributions of different anthropogenic volatile organic compound sources to ozone formation at a receptor site in the Pearl River Delta region and its policy implications, Atmos. Chem. Phys., 19, 8801-8816, https://doi.org/10.5194/acp-19-8801-2019, 2019.

Ho, K. F., Lee, S. C., Ho, W. K., Blake, D. R., Cheng, Y., Li, Y. S., Ho, S. S. H., Fung, K., Louie, P. K. K., and Park, D.: Vehicular emission of volatile organic compounds (VOCs) from a tunnel study in Hong Kong, Atmos. Chem. Phys., 9, 7491-7504, https://doi.org/10.5194/acp-9-7491-2009, 2009.

Houweling, S., Dentener, F., and Lelieveld, J.: The impact of nonmethane hydrocarbon compounds on tropospheric photochemistry, J. Geophys. Res.-Atmos., 103, 10673-10696, https://doi.org/10.1029/97JD03582, 1998.

Hui, L., Liu, X., Tan, Q., Feng, M., An, J., Qu, Y., Zhang, Y., and Jiang, M.: Characteristics, source apportionment and contribution of vocs to ozone formation in Wuhan, Central China, Atmos. Environ., 192, 55-71, https://doi.org/10.1016/j.atmosenv.2018.08.042, 2018.

Jobson, B. T., McKeen, S. A., Parrish, D. D., Fehsenfeld, F. C., Blake, D. R., Goldstein, A. H., Schauffler, S. M., and Elkins, J. C.: Trace gas mixing ratio variability versus lifetime in the troposphere and stratosphere: Observations, J. Geophys. Res.-Atmos., 104, 16091-16113, https://doi.org/10.1029/1999JD900126, 1999.

Jobson, B. T., Parrish, D. D., Goldan, P., Kuster, W., Fehsenfeld, F. C., Blake, D. R., Blake, N. J., and Niki, H.: Spatial and temporal variability of nonmethane hydrocarbon mixing ratios and

https://doi.org/10.5194/egusphere-2023-2935
Preprint. Discussion started: 6 March 2024

their relation to photochemical lifetime, J. Geophys. Res.-Atmos., 103, 13557-13567, https://doi.org/10.1029/97JD01715, 1998.

Jobson, B. T., Berkowitz, C. M., Kuster, W. C., Goldan, P. D., Williams, E. J., Fesenfeld, F. C., Apel, E. C., Karl, T., Lonneman, W. A., and Riemer, D.: Hydrocarbon source signatures in Houston, Texas: Influence of the petrochemical industry, J. Geophys. Res.-Atmos., 109, https://doi.org/10.1029/2004JD004887, 2004.

Kato, S., Pochanart, P., and Kajii, Y.: Measurements of ozone and nonmethane hydrocarbons at Chichi-jima island, a remote island in the Western Pacific: Long-range transport of polluted air from the Pacific rim region, Atmos. Environ., 35, 6021-6029, https://doi.org/10.1016/S1352-2310(01)00453-8, 2001.

Kato, S., Ui, T., Uematsu, M., and Kajii, Y.: Trace gas measurements over the Northwest Pacific during the 2002 IOC cruise, Geochem. Geophys. Geosyst., 8, https://doi.org/10.1029/2006GC001241, 2007.

Kato, S., Kajii, Y., Itokazu, R., Hirokawa, J., Koda, S., and Kinjo, Y.: Transport of atmospheric carbon monoxide, ozone, and hydrocarbons from Chinese coast to Okinawa island in the Western Pacific during winter, Atmos. Environ., 38, 2975-2981, https://doi.org/10.1016/j.atmosenv.2004.02.049, 2004.

Lai, S. C., Baker, A. K., Schuck, T. J., van Velthoven, P., Oram, D. E., Zahn, A., Hermann, M., Weigelt, A., Slemr, F., Brenninkmeijer, C. A. M., and Ziereis, H.: Pollution events observed during caribic flights in the upper troposphere between South China and the Philippines, Atmos. Chem. Phys., 10, 1649-1660, https://doi.org/10.5194/acp-10-1649-2010, 2010.

Lana, A., Bell, T. G., Simo, R., Vallina, S. M., Ballabrera-Poy, J., Kettle, A. J., Dachs, J., Bopp, L., Saltzman, E. S., Stefels, J., Johnson, J. E., and Liss, P. S.: An updated climatology of surface dimethlysulfide concentrations and emission fluxes in the global ocean, Glob. Biogeochem. Cycle, 25, https://doi.org/10.1029/2010GB003850, 2011.

Lee, C. L. and Brimblecombe, P.: Anthropogenic contributions to global carbonyl sulfide, carbon disulfide and organosulfides fluxes, Earth-Sci. Rev., 160, 1-18, https://doi.org/10.1016/j.earscirev.2016.06.005, 2016.

Lee, R. F. and Baker, J.: Ethylene and ethane production in an estuarine river: Formation from the

https://doi.org/10.5194/egusphere-2023-2935
Preprint. Discussion started: 6 March 2024

decomposition of polyunsaturated fatty acids, Mar. Chem., 38, 25-36, https://doi.org/10.1016/0304-4203(92)90065-I, 1992.

Li, J. L., Zhai, X., Ma, Z., Zhang, H. H., and Yang, G. P.: Spatial distributions and sea-to-air fluxes of non-methane hydrocarbons in the atmosphere and seawater of the Western Pacific Ocean, Sci. Total Environ., 672, 491-501, https://doi.org/10.1016/j.scitotenv.2019.04.019, 2019.

Li, J. L., Zhai, X., Wu, Y. C., Wang, J., Zhang, H. H., and Yang, G. P.: Emissions and potential controls of light alkenes from the marginal seas of China, Sci. Total Environ., 758, https://doi.org/10.1016/j.scitotenv.2020.143655, 2021.

Li, L. Y., Xie, S. D., Zeng, L. M., Wu, R. R., and Li, J.: Characteristics of volatile organic compounds and their role in ground-level ozone formation in the Beijing-Tianjin-Hebei region, China, Atmos. Environ., 113, 247-254, https://doi.org/10.1016/j.atmosenv.2015.05.021, 2015.

Liu, B. S., Liang, D. N., Yang, J. M., Dai, Q. L., Bi, X. H., Feng, Y. C., Yuan, J., Xiao, Z. M., Zhang, Y. F., and Xu, H.: Characterization and source apportionment of volatile organic compounds based on 1-year of observational data in Tianjin, China, Environ. Pollut., 218, 757-769, https://doi.org/10.1016/j.envpol.2016.07.072, 2016.

Liu, Y., Shao, M., Fu, L., Lu, S., Zeng, L., and Tang, D.: Source profiles of volatile organic compounds (VOCs) measured in China: Part i, Atmos. Environ., 42, 6247-6260, https://doi.org/10.1016/j.atmosenv.2008.01.070, 2008.

Mallik, C., Lal, S., Venkataramani, S., Naja, M., and Ojha, N.: Variability in ozone and its precursors over the bay of Bengal during post monsoon: Transport and emission effects, J. Geophys. Res.-Atmos., 118, 10190-10209, https://doi.org/10.1002/jgrd.50764, 2013.

Paatero, P. and Tapper, U.: Positive matrix factorization - a nonnegative factor model with optimal utilization of error-estimates of data values, Environmetrics, 5, 111-126, https://doi.org/10.1002/env.3170050203, 1994.

Parrish, D. D., Kuster, W. C., Shao, M., Yokouchi, Y., Kondo, Y., Goldan, P. D., de Gouw, J. A., Koike, M., and Shirai, T.: Comparison of air pollutant emissions among mega-cities, Atmos. Environ., 43, 6435-6441, https://doi.org/10.1016/j.atmosenv.2009.06.024, 2009.

Quack, B. and Wallace, D. W. R.: Air-sea flux of bromoform: Controls, rates, and implications, Glob. Biogeochem. Cycle, 17, https://doi.org/10.1029/2002GB001890, 2003.

https://doi.org/10.5194/egusphere-2023-2935
Preprint. Discussion started: 6 March 2024

Ratte, M., Plassdulmer, C., Koppmann, R., and Rudolph, J.: Horizontal and vertical profiles of light-hydrocarbons in sea-water related to biological, chemical and physical parameters, Tellus Ser. B-Chem. Phys. Meteorol., 47, 607-623, https://doi.org/10.1034/j.1600-0889.47.issue5.8.x, 1995.

Ratte, M., Plassdulmer, C., Koppmann, R., Rudolph, J., and Denga, J.: Production mechanism of c2-c4 hydrocarbons in seawater - field-measurements and experiments, Glob. Biogeochem. Cycle, 7, 369-378, https://doi.org/10.1029/93gb00054, 1993.

Riemer, D. D., Milne, P. J., Zika, R. G., and Pos, W. H.: Photoproduction of nonmethane hydrocarbons (NMHCs) in seawater, Mar. Chem., 71, 177-198, https://doi.org/10.1016/S0304-4203(00)00048-7, 2000.

Rossabi, S. and Helmig, D.: Changes in atmospheric butanes and pentanes and their isomeric ratios in the continental United States, J. Geophys. Res.-Atmos., 123, 3772-3790, https://doi.org/10.1002/2017JD027709, 2018.

Rudolph, J. and Johnen, F. J.: Measurements of light atmospheric hydrocarbons over the Atlantic in regions of low biological activity, J. Geophys. Res.-Atmos., 95, 20583-20591, https://doi.org/10.1029/JD095iD12p20583, 1990.

Russo, R. S., Zhou, Y., White, M. L., Mao, H., Talbot, R., and Sive, B. C.: Multi-year (2004–2008) record of nonmethane hydrocarbons and halocarbons in New England: Seasonal variations and regional sources, Atmos. Chem. Phys., 10, 4909-4929, https://doi.org/10.5194/acp-10-4909-2010, 2010.

Russo, R. S., Talbot, R. W., Dibb, J. E., Scheuer, E., Seid, G., Jordan, C. E., Fuelberg, H. E., Sachse, G. W., Avery, M. A., Vay, S. A., Blake, D. R., Blake, N. J., Atlas, E., Fried, A., Sandholm, S. T., Tan, D., Singh, H. B., Snow, J., and Heikes, B. G.: Chemical composition of Asian continental outflow over the Western Pacific: Results from Transport and Chemical Evolution over the Pacific (TRACE-P), J. Geophys. Res.-Atmos., 108, https://doi.org/10.1029/2002JD003184, 2003.

Sahu, L. K., Lal, S., and Venkataramani, S.: Impact of monsoon circulations on oceanic emissions of light alkenes over bay of Bengal, Glob. Biogeochem. Cycle, 24, https://doi.org/10.1029/2009GB003766, 2010.

https://doi.org/10.5194/egusphere-2023-2935
Preprint. Discussion started: 6 March 2024

705 Sahu, L. K., Lal, S., and Venkataramani, S.: Seasonality in the latitudinal distributions of NMHCs
706 over bay of Bengal, Atmos. Environ., 45, 2356-2366,
707 https://doi.org/10.1016/j.atmosenv.2011.02.021, 2011.
708 Solomon, S., Thompson, D. W. J., Portmann, R. W., Oltmans, S. J., and Thompson, A. M.: On the
709 distribution and variability of ozone in the tropical upper troposphere: Implications for tropical
710 deep convection and chemical-dynamical coupling, Geophys. Res. Lett., 32,
711 https://doi.org/10.1029/2005GL024323, 2005.
712 Song, J. W., Zhang, Y. Y., Zhang, Y. L., Yuan, Q., Zhao, Y., Wang, X. M., Zou, S. C., Xu, W. H., and
713 Lai, S. C.: A case study on the characterization of non-methane hydrocarbons over the South
714 China Sea: Implication of land-sea air exchange, Sci. Total Environ., 717,
715 https://doi.org/10.1016/j.scitotenv.2019.134754, 2020.
716 Song, Y., Shao, M., Liu, Y., Lu, S. H., Kuster, W., Goldan, P., and Xie, S. D.: Source apportionment
717 of ambient volatile organic compounds in Beijing, Environ. Sci. Technol., 41, 4348-4353,
718 https://doi.org/10.1021/es0625982, 2007.
719 Swarthout, R. F., Russo, R. S., Zhou, Y., Hart, A. H., and Sive, B. C.: Volatile organic compound
720 distributions during the NACHTT campaign at the Boulder Atmospheric Observatory:
721 Influence of urban and natural gas sources, J. Geophys. Res.-Atmos., 118, 10,614-610,637,
722 https://doi.org/10.1002/jgrd.50722, 2013.
723 Talbot, R., Dibb, J., Scheuer, E., Seid, G., Russo, R., Sandholm, S., Tan, D., Singh, H., Blake, D.,
724 Blake, N., Atlas, E., Sachse, G., Jordan, C., and Avery, M.: Reactive nitrogen in Asian
725 continental outflow over the western Pacific: Results from the NASA Transport and Chemical
726 Evolution over the Pacific (TRACE-P) airborne mission, J. Geophys. Res.-Atmos., 108,
727 https://doi.org/10.1029/2002JD003129, 2003.
728 Tang, J. H., Chan, L. Y., Chang, C. C., Liu, S., and Li, Y. S.: Characteristics and sources of non-
729 methane hydrocarbons in background atmospheres of eastern, southwestern, and southern
730 China, J. Geophys. Res.-Atmos., 114, https://doi.org/10.1029/2008JD010333, 2009.
731 Tran, S., Bonsang, B., Gros, V., Peeken, I., Sarda-Esteve, R., Bernhardt, A., and Belviso, S.: A survey
732 of carbon monoxide and non-methane hydrocarbons in the Arctic Ocean during summer 2010,
733 Biogeosciences, 10, 1909-1935, https://doi.org/10.5194/bg-10-1909-2013, 2013.

https://doi.org/10.5194/egusphere-2023-2935
Preprint. Discussion started: 6 March 2024

734 Tsai, W. Y., Chan, L. Y., Blake, D. R., and Chu, K. W.: Vehicular fuel composition and atmospheric
735 emissions in South China: Hong Kong, Macau, Guangzhou, and Zhuhai, Atmos. Chem. Phys.,
736 6, 3281-3288, https://doi.org/10.5194/acp-6-3281-2006, 2006.
737 Wang, T., Ding, A. J., Blake, D. R., Zahorowski, W., Poon, C. N., and Li, Y. S.: Chemical
738 characterization of the boundary layer outflow of air pollution to Hong Kong during february-
739 april 2001, J. Geophys. Res.-Atmos., 108, https://doi.org/10.1029/2002JD003272, 2003.
740 Wang, T., Guo, H., Blake, D. R., Kwok, Y. H., Simpson, I. J., and Li, Y. S.: Measurements of trace
741 gases in the inflow of South China Sea background air and outflow of regional pollution at Tai
742 O, Southern China, J. Atmos. Chem., 52, 295-317, https://doi.org/10.1007/s10874-005-2219-
743 x, 2005.
744 Wanninkhof, R.: Relationship between wind-speed and gas-exchange over the ocean, J. Geophys.
745 Res.-Oceans, 97, 7373-7382, https://doi.org/10.1029/92jc00188, 1992.
746 Warneke, C. and de Gouw, J. A.: Organic trace gas composition of the marine boundary layer over
747 the Northwest Indian Ocean in april 2000, Atmos. Environ., 35, 5923-5933,
748 https://doi.org/10.1016/S1352-2310(01)00384-3, 2001.
749 Wilke, C. R. and Chang, P.: Correlation of diffusion coefficients in dilute solutions, AIChE Journal,
750 1, 264-270, https://doi.org/10.1002/aic.690010222, 1955.
751 Willis, M. D., Köllner, F., Burkart, J., Bozem, H., Thomas, J. L., Schneider, J., Aliabadi, A. A., Hoor,
752 P. M., Schulz, H., Herber, A. B., Leaitch, W. R., and Abbatt, J. P. D.: Evidence for marine
753 biogenic influence on summertime arctic aerosol, Geophys. Res. Lett., 44, 6460-6470,
754 https://doi.org/10.1002/2017GL073359, 2017.
755 Wong, H. L. A., Wang, T., Ding, A., Blake, D. R., and Nam, J. C.: Impact of Asian continental
756 outflow on the concentrations of O3, CO, NMHCs and halocarbons on Jeju Island, South Korea
757 during march 2005, Atmos. Environ., 41, 2933-2944,
758 https://doi.org/10.1016/j.atmosenv.2006.12.030, 2007.
759 Wu, D., Ding, X., Li, Q., Sun, J., Huang, C., Yao, L., Wang, X., Ye, X., Chen, Y., He, H., and Chen,
760 J.: Pollutants emitted from typical Chinese vessels: Potential contributions to ozone and
761 secondary organic aerosols, J. Clean. Prod., 238, 117862,
762 https://doi.org/10.1016/j.jclepro.2019.117862, 2019.

https://doi.org/10.5194/egusphere-2023-2935
Preprint. Discussion started: 6 March 2024

763 Wu, F., Yu, Y., Sun, J., Zhang, J., Wang, J., Tang, G., and Wang, Y.: Characteristics, source
764 apportionment and reactivity of ambient volatile organic compounds at Dinghu Mountain in
765 Guangdong Province, China, Sci. Total Environ., 548-549, 347-359,
766 https://doi.org/10.1016/j.scitotenv.2015.11.069, 2016.
767 Wu, R. R. and Xie, S. D.: Spatial distribution of secondary organic aerosol formation potential in
768 China derived from speciated anthropogenic volatile organic compound emissions, Environ.
769 Sci. Technol., 52, 8146-8156, https://doi.org/10.1021/acs.est.8b01269, 2018.
770 Wu, Y. C., Li, J. L., Wang, J., Zhuang, G. C., Liu, X. T., Zhang, H. H., and Yang, G. P.: Occurance,
771 emission and environmental effects of non-methane hydrocarbons in the Yellow Sea and the
772 East China Sea, Environ. Pollut., 270, 12, https://doi.org/10.1016/j.envpol.2020.116305, 2021.
773 Wu, Y. C., Gao, X. X., Zhang, H. H., Liu, Y. Z., Wang, J., Xu, F., Zhang, G. L., and Chen, Z. H.:
774 Characteristics and emissions of isoprene and other non-methane hydrocarbons in the
775 Northwest Pacific Ocean and responses to atmospheric aerosol deposition, Sci. Total Environ.,
776 876, https://doi.org/10.1016/j.scitotenv.2023.162808, 2023.
777 Xiao, Q., Li, M., Liu, H., Fu, M., Deng, F., Lv, Z., Man, H., Jin, X., Liu, S., and He, K.:
778 Characteristics of marine shipping emissions at berth: Profiles for particulate matter and
779 volatile organic compounds, Atmos. Chem. Phys., 18, 9527-9545, https://doi.org/10.5194/acp-
780 18-9527-2018, 2018a.
781 Xiao, Q., Li, M., Liu, H., Fu, M. L., Deng, F. Y., Lv, Z. F., Man, H. Y., Jin, X. X., Liu, S., and He,
782 K. B.: Characteristics of marine shipping emissions at berth: Profiles for particulate matter and
783 volatile organic compounds, Atmos. Chem. Phys., 18, 9527-9545, https://doi.org/10.5194/acp-
784 18-9527-2018, 2018b.
785 Yuan, Q., Lai, S. C., Song, J. W., Ding, X., Zheng, L. S., Wang, X. M., Zhao, Y., Zheng, J. Y., Yue,
786 D. L., Zhong, L. J., Niu, X. J., and Zhang, Y. Y.: Seasonal cycles of secondary organic aerosol
787 tracers in rural Guangzhou, Southern China: The importance of atmospheric oxidants, Environ.
788 Pollut., 240, 884-893, https://doi.org/10.1016/j.envpol.2018.05.009, 2018.
789 Zhang, Y., Zhi, Z., Li, X., Gao, J., and Song, Y.: Carboxylated mesoporous carbon microparticles as
790 new approach to improve the oral bioavailability of poorly water-soluble carvedilol, Int. J.
791 Pharm., 454, 403-411, https://doi.org/10.1016/j.ijpharm.2013.07.009, 2013.

https://doi.org/10.5194/egusphere-2023-2935
Preprint. Discussion started: 6 March 2024

Zhang, Y., Wang, X., Zhang, Z., Lü, S., Huang, Z., and Li, L.: Sources of c2–c4 alkenes, the most important ozone nonmethane hydrocarbon precursors in the Pearl River Delta region, Sci. Total Environ., 502, 236-245, https://doi.org/10.1016/j.scitotenv.2014.09.024, 2015.

Zhang, Z., Zhang, Y., Wang, X., Lü, S., Huang, Z., Huang, X., Yang, W., Wang, Y., and Zhang, Q.: Spatiotemporal patterns and source implications of aromatic hydrocarbons at six rural sites across China's developed coastal regions, J. Geophys. Res.-Atmos., 121, 6669-6687, https://doi.org/10.1002/2016JD025115, 2016.

Zhang, Z. J., Yan, X. Y., Gao, F. L., Thai, P., Wang, H., Chen, D., Zhou, L., Gong, D. C., Li, Q. Q., Morawska, L., and Wang, B. G.: Emission and health risk assessment of volatile organic compounds in various processes of a petroleum refinery in the Pearl River Delta, China, Environ. Pollut., 238, 452-461, https://doi.org/10.1016/j.envpol.2018.03.054, 2018.

Zhou, S. Q., Chen, Y., Paytan, A., Li, H. W., Wang, F. H., Zhu, Y. C., Yang, T. J., Zhang, Y., and Zhang, R. F.: Non-marine sources contribute to aerosol methanesulfonate over coastal seas, J. Geophys. Res.-Atmos., 126, https://doi.org/10.1029/2021JD034960, 2021.

Zou, Y. W., He, Z., Liu, C. Y., Qi, Q. Q., Yang, G. P., and Mao, S. H.: Coastal observation of halocarbons in the yellow sea and east china sea during winter: Spatial distribution and influence of different factors on the enzyme-mediated reactions, Environ. Pollut., 290, https://doi.org/10.1016/j.envpol.2021.118022, 2021.

https://doi.org/10.5194/egusphere-2023-2935
Preprint. Discussion started: 6 March 2024

Figure Captions

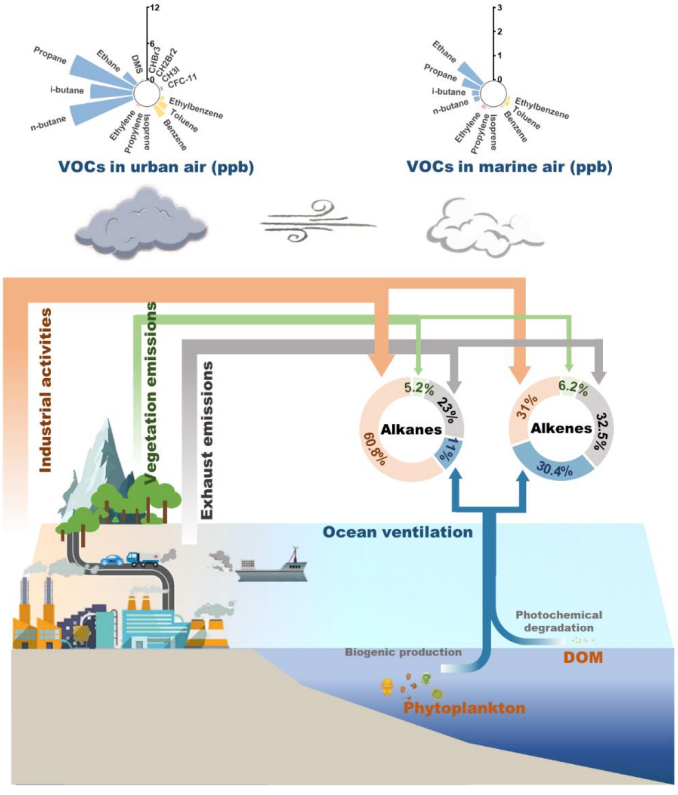

Graphical abstract Schematic diagram showing the main sources and their relative contributions to the non-methane hydrocarbons (NMHCs) budget in the nearshore atmospheres of China. The ring bar chart above the land or the ocean shows the composition of urban or marine atmospheric trace gases determined in this study. The axes with unit of ppb indicate the atmospheric concentrations of gases. The distinct colored wedges indicate the alkanes (skyblue), alkenes (pink), monocyclic aromatics (yellow), volatile halogenated compounds (VHCs, lilac), and dimethyl sulfur (DMS, palegreen). Note that only alkanes, alkenes, and monocyclic aromatics are shown in marine atmosphere. The colored arrows or annuli indicate the main sources of NMHCs in offshore atmosphere: industrial activities (sandybrown), exhaust emissions (darkgray), oceanic ventilation (steelblue), and vegetation emissions (lightgreen). The numbers on the annuli are their respective relative contributions.

https://doi.org/10.5194/egusphere-2023-2935
Preprint. Discussion started: 6 March 2024

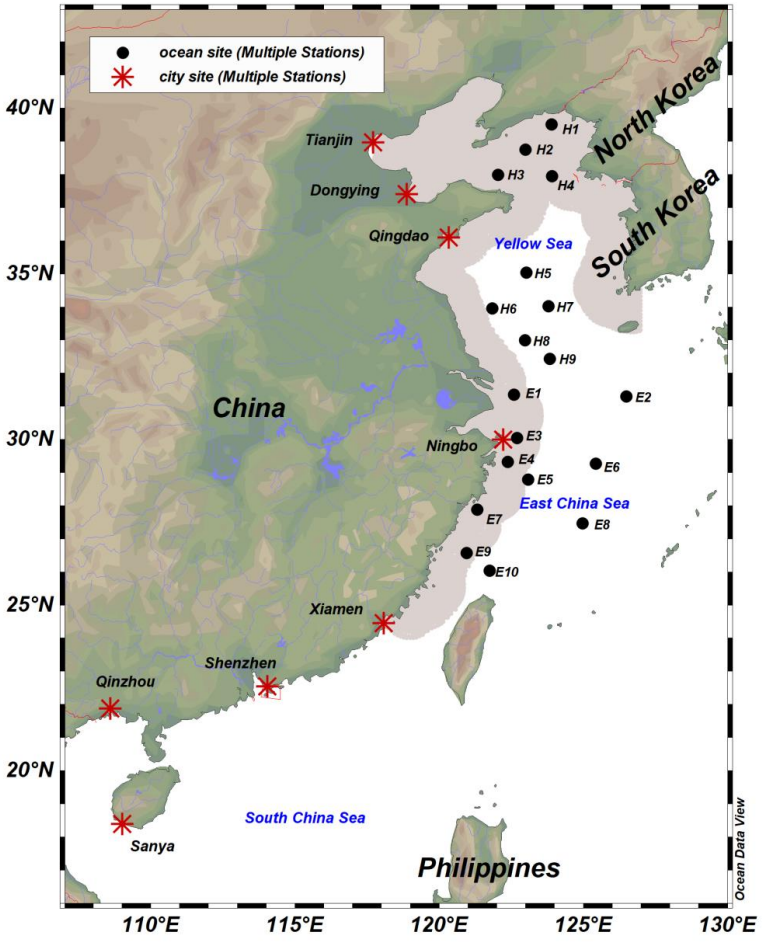

Figure 1 Map showing the sampling stations in the coastal cities (red asterisks) and marginal seas (black dots) of China from March to May 2021. The gray shaded area represents the inshore region within 100 km from the coastline.

https://doi.org/10.5194/egusphere-2023-2935
Preprint. Discussion started: 6 March 2024

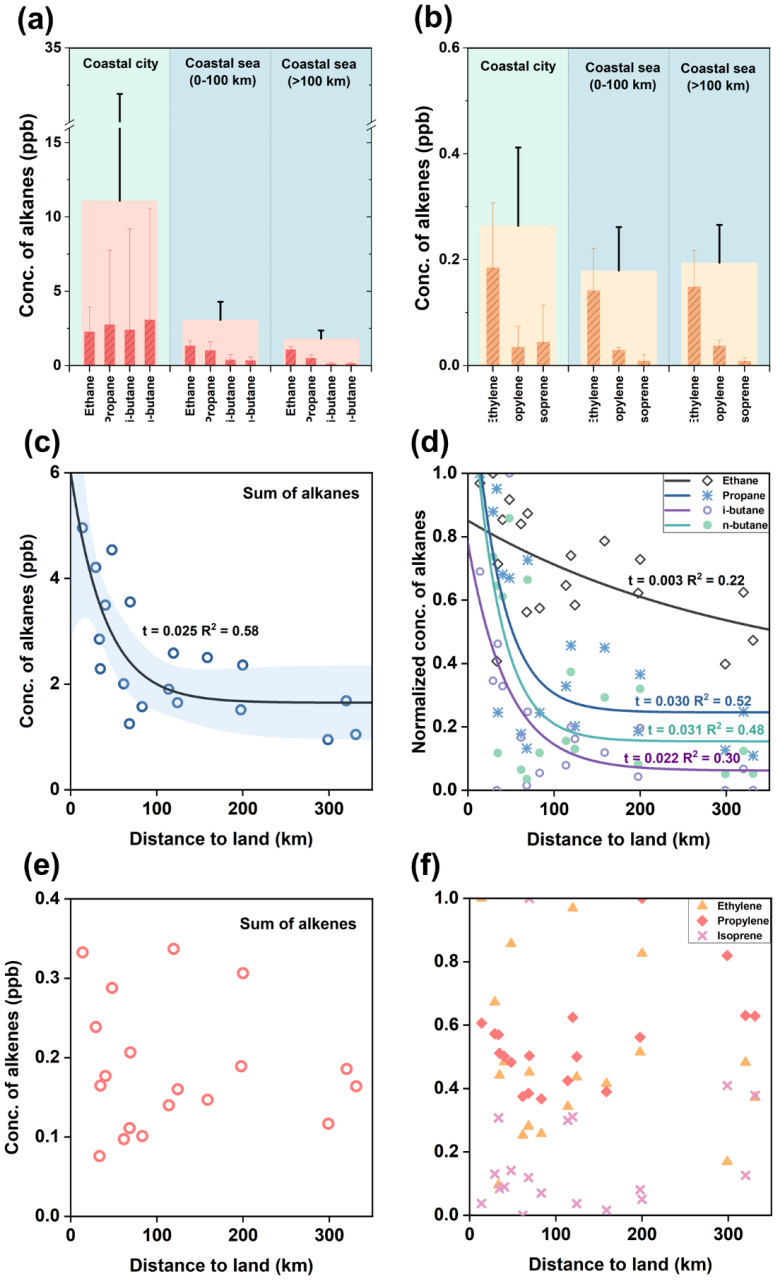

833

834 **Figure 2** Means of the concentrations of alkanes (panel a) and alkenes (panel b) in the atmosphere

835 over coastal cities (n = 14) and nearshore (0-100 km, n = 10) and offshore (>100 km, n = 9) coastal

https://doi.org/10.5194/egusphere-2023-2935
Preprint. Discussion started: 6 March 2024

836 seas of China. The wider columns in panel a or b represent the sums of individual alkanes or alkenes
837 with error bars depicting the propagated errors from each NMHCs. Summed alkane (panel c) or
838 alkene (panel e) and normalized concentrations of specific alkane (panel d) or alkene (panel f)
839 plotted as a function ($y = Ae^{-t\tau}+y_0$) of the distance from sampling sites to the nearest land.
840

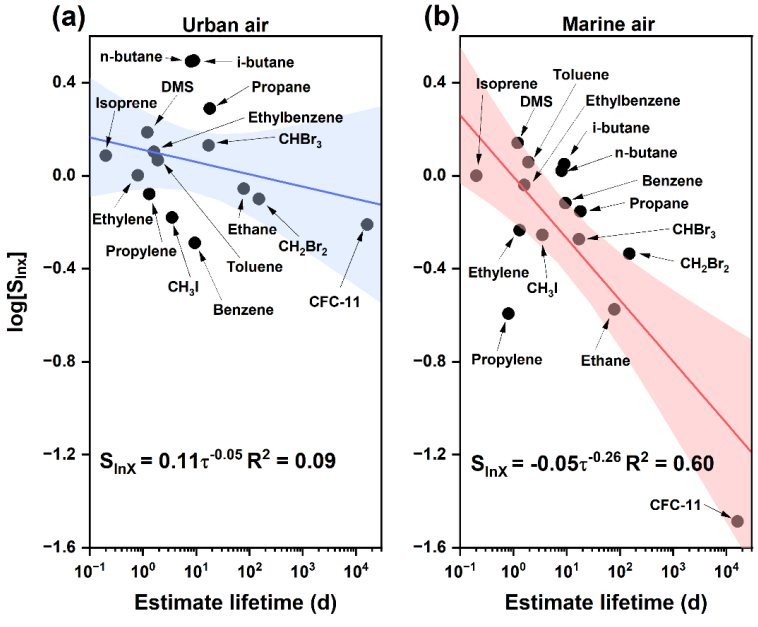

841

842 **Figure 3** Atmospheric variability (log[S_{lnx}]) plotted as a function of the estimated •OH lifetime for
843 each non-methane hydrocarbons (NMHCs) from the coastal cities (panel a) and marginal seas of
844 China (panel b). The blue or red line is the best linear fitting. Shadowed area represents the
845 confidence band at a 95 % confidence level.

https://doi.org/10.5194/egusphere-2023-2935
Preprint. Discussion started: 6 March 2024

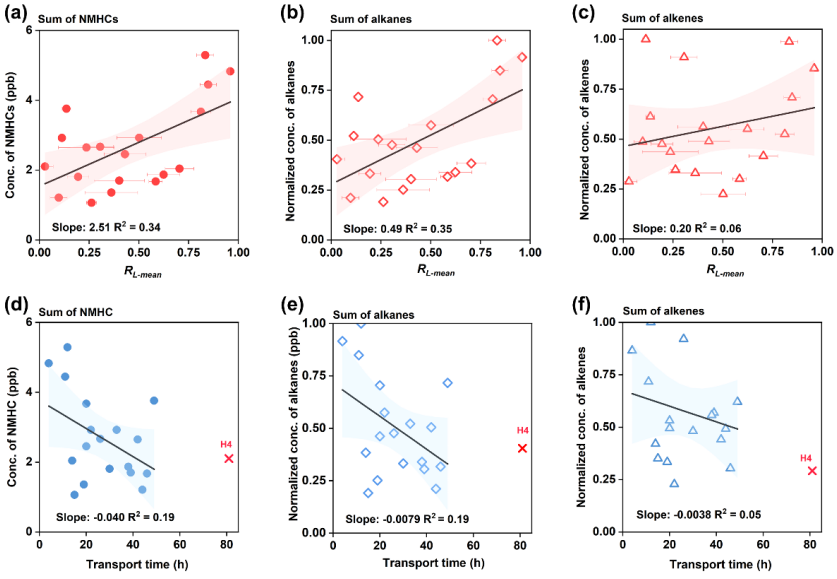

Figure 4 Concentrations of non-methane hydrocarbons (NMHCs) combined (panel a or d), alkanes (panel b or e), and alkenes (panel c or f) at each site plotted against the mean retentions of air mass over land (R_{L-mean}, n = 3) or the transport time of air mass, respectively. The error bars for R_{L-mean} indicate the standard deviation from three different time-scale trajectories (48h, 72h, and 96h). The black line is the best fitting of liner function and shadowed area represents the confidence band at a 95 % confidence level. H4 (marked with red "×") is treated as an outlier since it alone deviates from the main dataset.

https://doi.org/10.5194/egusphere-2023-2935
Preprint. Discussion started: 6 March 2024

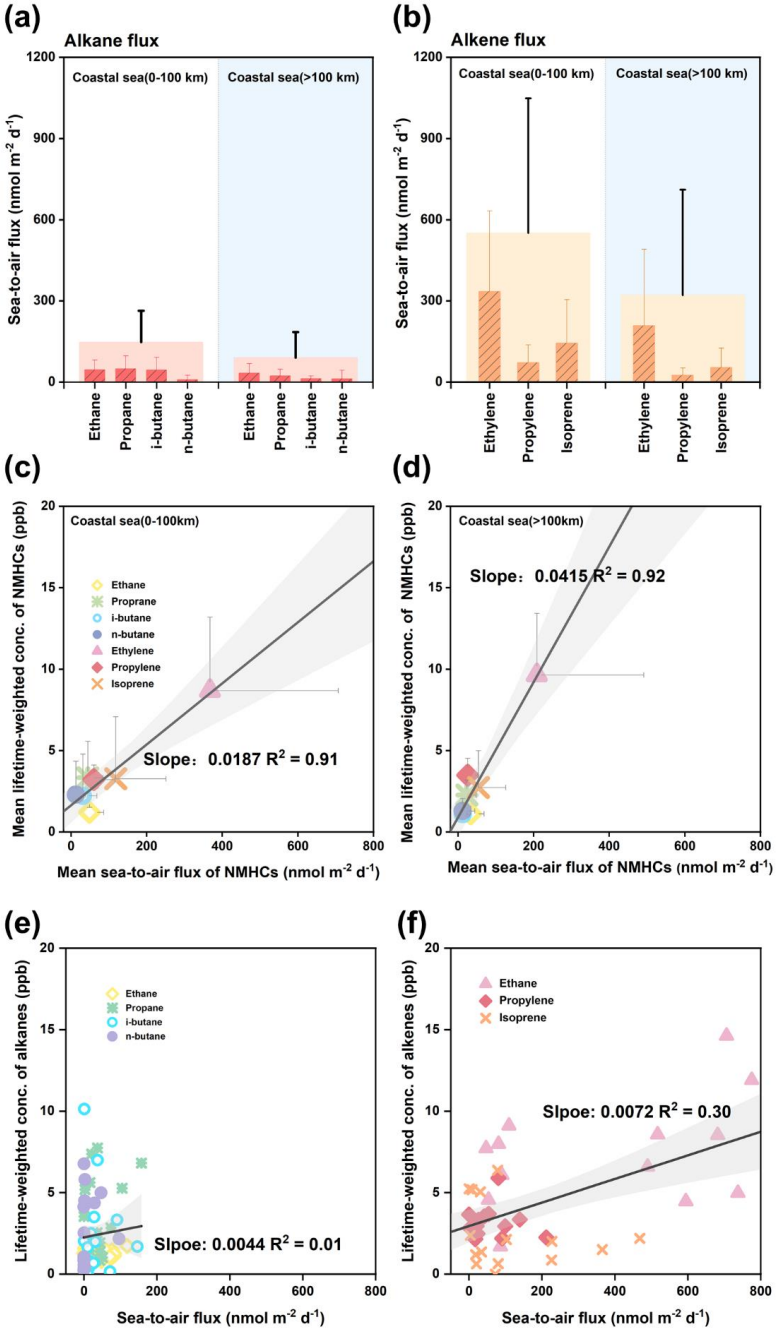

Figure 5 Means of sea-to-air fluxes of alkanes (panel a) and alkenes (panel b) in sea areas within 100 km (n = 10) and beyond 100 km (n = 9) from the nearshore land. The wider columns represent

https://doi.org/10.5194/egusphere-2023-2935
Preprint. Discussion started: 6 March 2024

the sum of alkanes or alkenes. Panel c or d shows the means of lifetime-weighted concentrations of NMHCs plotted against the means of their mean sea-to-air fluxes in the area within 100 km or beyond 100 km from the coastline. Specific lifetime-weighted concentrations of alkanes (panel e) and alkenes (panel f) plotted against sea-to-air fluxes in the whole coastal sea region. The black, blue or red line is the best linear fitting for each dataset and shadowed area represents the confidence band at a 95 % confidence level.

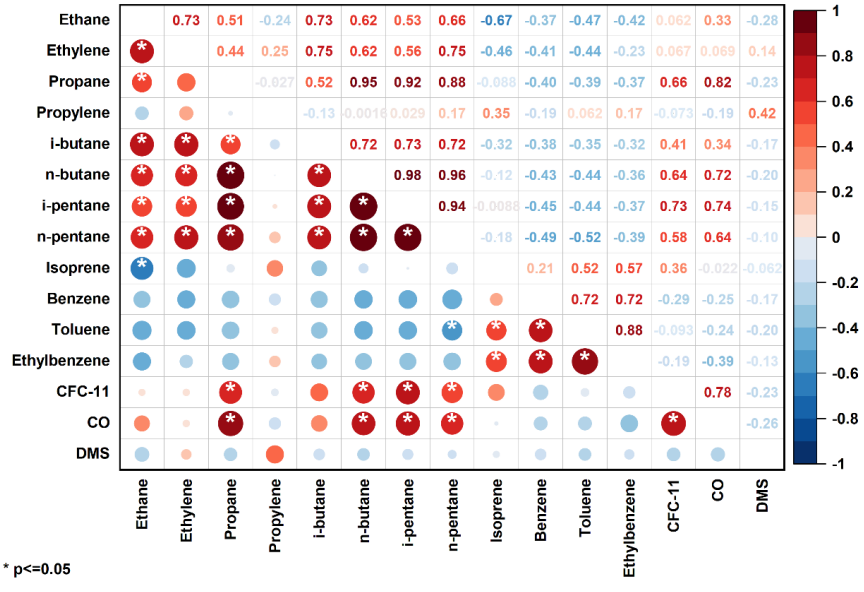

Figure 6 Correlation coefficients (r) between the various trace gases determined in the atmosphere over the Yellow Sea and the East China Sea. The white asterisk means the correlation is significant at the $p<0.05$ level. The color of dots, red or blue, indicates the positive or negative correlation and the size of the dots indicates the absolute value of r.

https://doi.org/10.5194/egusphere-2023-2935
Preprint. Discussion started: 6 March 2024

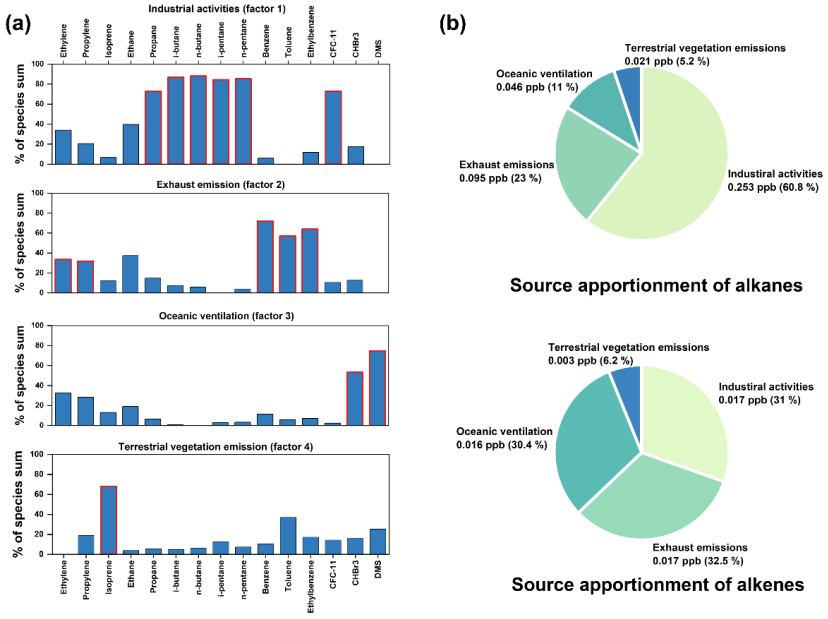

869

870 **Figure 7** Representative factor profiles from the positive matrix factorization (PMF) model (panel
871 a). Non-methane hydrocarbons (NMHCs) marked with red rim are selected as indicators for the
872 specific factors. Relative contributions of different factors/sources to the alkanes and alkenes in the
873 oceanic atmosphere (panel b).

Table

Table 1 Atmospheric and seawater concentrations, sea-to-air fluxes, and the calculated atmospheric lifetime of each non-methane hydrocarbons (NMHCs) based on the reaction with hydroxyl radicals (•OH).

Species	Conc. in urban air (ppb)	Conc. in oceanic air (ppb)	Conc. in seawater (pmol L^{-1})	Sea-to-air flux (nmol m^{-2} d^{-1})	Atmospheric lifetime [b] (d)
Ethane	2.26 (0.277-5.72)	1.24 (0.686-1.72)	11.6 (4.70-22.8)	44.6 (0.2-118)	78
Propane	2.95 (0.149-20.1)	0.822 (0.226-1.79)	12.6 (3.68-136)	41.5 (0.2-157)	18
i-butane	2.57 (BD [a]-27.6)	0.283 (BD-1.17)	9.46 (1.54-35.3)	31.7 (0.1-146)	9.1
n-butane	3.29 (0.018-30.2)	0.256 (0.025-0.694)	4.95 (BD-32.9)	10.9 (-0.8-96.1)	8.2
Ethylene	0.180 (0.035-0.390)	0.151 (0.028-0.295)	70.4 (8.40-136)	321 (1.7-775)	2.3
Propylene	0.036 (BD-0.129)	0.033 (0.022-0.060)	15.2 (2.42-27.6)	56.1 (0.2-212)	0.73
Isoprene	0.046 (0.006-0.250)	0.008 (BD-0.043)	31.0 (3.43-105)	112 (0.5-468)	0.19

[a]: Below the detection limit.

[b]: Assuming an average [•OH] of 6×10^5 molecules cm^{-3} within 24 h (Jobson et al., 1999), and using the rate constant with •OH at 288 K taken from Atkinson et al. (1997).